Secular bathymetric variations of the North Channel in the Changjiang (Yangtze) Estuary, China, 1880–2013: Causes and effects

Xuefei Mei[a]

Zhijun Dai[a, b, *]
zjdai@sklec.ecnu.edu.cn

Wen Wei[a]

Weihua Li[a]

Jie Wang[a]

Hao Sheng[c]

[a]State Key Laboratory of Estuarine and Coastal Research, East China Normal University, Shanghai, 200062, China

[b]Laboratory for Marine Geology, Qingdao National Laboratory for Marine Science and Technology, Qingdao 266061, China

[c]Shanghai Waterway Engineering Design and Consulting Co., Ltd., Shanghai, 200120, China

*Corresponding author at: State Key Laboratory of Estuarine and Coastal Research, East China Normal University, Shanghai, China.

Abstract

As the interface between the fluvial upland system and the open coast, global estuaries are facing serious challenges owing to various anthropogenic activities, especially to the Changjiang Estuary. Since the establishment of the Three Gorges Dam (TGD), currently the world's largest hydraulic structure, and certain other local hydraulic engineering structures, the Changjiang Estuary has experienced severe bathymetric variations. It is urgent to analyze the estuarine morphological response to the basin-wide disturbance to enable a better management of estuarine environments. North Channel (NC), the largest anabranched estuary in the Changjiang Estuary, is the focus of this study. Based on the analysis of bathymetric data between 1880 and 2013 and related hydrological data, we developed the first study on the centennial bathymetric variations of the NC. It is found that the bathymetric changes of NC include two main modes, with the first mode representing 64% of the NC variability, which indicates observable deposition in the mouth bar and its outer side area (lower reach); the second mode representing 11% of the NC variability, which further demonstrates channel deepening along the inner side of the mouth bar (upper reach) during 1970–2013. Further, recent erosion observed along the inner side of the mouth bar is caused by riverine sediment decrease, especially in relation to TGD induced sediment trapping since 2003, while the deposition along the lower reach since 2003 can be explained by the landward sediment transport because of flood-tide force strengthen under the joint action of TGD induced seasonal flood discharge decrease and land reclamation induced lower reach narrowing. Generally, the upper and lower NC reach are respectively dominated by fluvial and tidal discharge, however, episodic extreme floods can completely alter the channel morphology by smoothing the entire channel. The results presented herein for the NC enrich our understanding of bathymetric variations of the Changjiang Estuary in response to human activities, which can be well applied to other estuaries subject to similar interferences.

Keywords: Bathymetric variations; tThe North Channel; Suspended sediment discharge; Three Ggorges Ddam; Morphodynamic process

1.1 Introduction

As the interfaces between fluvial upland systems and wave-or tidal-dominated regimes of the open coast (Wright and Coleman, 1974; Liu et al., 2007), estuaries with continuously migrating channels and bars are commonly of great ecologic and socio-economic significance and, as such, their management is of crucial importance. However, estuarine systems are being put under increasing pressure by natural and anthropogenic disturbances, which have substantially affected their bathymetric evolution (Anthony et al., 2014, 2015; Fagherazzi et al., 2006; Syvitski and Saito, 2007). An in-depth knowledge of estuarine bathymetric variations and the governing mechanisms of their morphodynamic evolution is essential for the sustainable management of estuarine environments and related policy making (Coco et al., 2013; Anthony et al., 2014; Dai et al., 2014).

Naturally, bathymetric variations of an estuary strongly depend on the relative influence of the river, waves and tides at the river mouth (Wright and Coleman, 1973). However, basin-wide hydrologic engineering, notably large-capacity dams, can dramatically affect estuarine morphology by changing the fluvial water and sediment supply to the estuary. For instance, Wolanski et al. (2001) observed considerable siltation in the East Arm of Cambridge Gulf, Australia, as a result of dam-induced suppression of large river floods and hence a greater amount of marine sediment delivery into the East Arm. Similarly, the sedimentation rate in the Keum River Estuary, southern Korea, increased by a factor of 1.9, after dam construction in the upper reaches (Kim et al., 2006). There are also many examples of estuaries and deltas undergoing erosion problems caused by damming induced riverine sediment load reduction. A typical example is the Mississippi River, which lost 25% of its deltaic wetlands to the ocean because of dam construction in the river basin (Blum and Roberts, 2009). The construction of reservoirs has also contributed to the severe shoal erosion and coastline retreat in rivers of the Mediterranean coast (Bergillos et al., 2016).

While river damming can alter the morphology of river estuaries, other human activities, such as channel deviation, dredging, deforestation, or land reclamation, have also significantly modified the estuarine environment. For example, many estuaries in Spain experienced a drastic reduction of their intertidal zones in the nineteenth and twentieth centuries due to drying and filling of these areas (Jiménez et al., 2012). UK estuaries have been affected to varying degrees by embanking, land reclamation, dredging under various tidal and wave conditions, which thereafter adjusted quickly to present sedimentary infilling or erosion and sediment loss (Pye and Blott, 2014; Robins et al., 2016). Thomas et al. (2002) and Lane (2004) indicated that the volume of the Mersey Estuary decreased by 10% between 1906 and 1997 owing to the combined effects of training wall construction and dredging activity in the sea approach channels. Garel et al. (2014) indicated that the Guadiana estuary (southern Portugal) is in an immature state and stressed that the estuary's geomorphic response to jetty construction must be considered at multiple temporal and spatial scales. Estuarine systems therefore show complex bathymetric responses to hydraulic engineering projects.

The Changjiang Estuary (Fig. 1), as the largest bifurcated estuary in Asia, has been subject to extensive human interferences from both the upstream drainage basin, and within the estuary itself over the past 50 years. More than ≥ 50,000 dams have been constructed along the Changjiang River, which have resulted in a dramatic decline in riverine sediment discharge into the estuarine environment (Chen et al., 2010; Lai et al., 2017). In particular, following the establishment of the Three Gorges Dam (TGD) in 2003, currently the world's largest river engineering project, riverine sediment from the Changjiang River to the East China Sea has decreased by approximately 70% relative to the period

1950–1968 (Yang et al., 2015; Dai et al., 2016a, 2016b). Meanwhile, local human activities, such as land reclamation, sand extraction, marsh planting and navigational projects, provide additional pressure to the estuarine system (Wang et al., 2008a; Jiang et al., 2012). Although several studies have investigated the morphological evolution of the Changjiang Estuary in response to these basin-wide anthropologic activities, their results are still under debate. For example, Yang et al. (2010) indicated that 50,000 dams throughout the Changjiang River watershed resulted in erosion of the river's subaqueous delta. Luan et al. (2016) showed that the inner estuary altered from a state of sedimentation to a state of erosion in response to the river sediment decline while the mouth bar area showed continued accretion under the dominance of tidal forcing. In contrast, Dai et al. (2013, 2015, 2016) detected infilling in the North Branch, North Passage and South Passage, three distributaries of the Changjiang Estuary. Consequently, there is no consistent conclusion on the estuarine evolution in response to the engineering interferences and, in particular, to the North Channel (NC), which is still poorly understood.
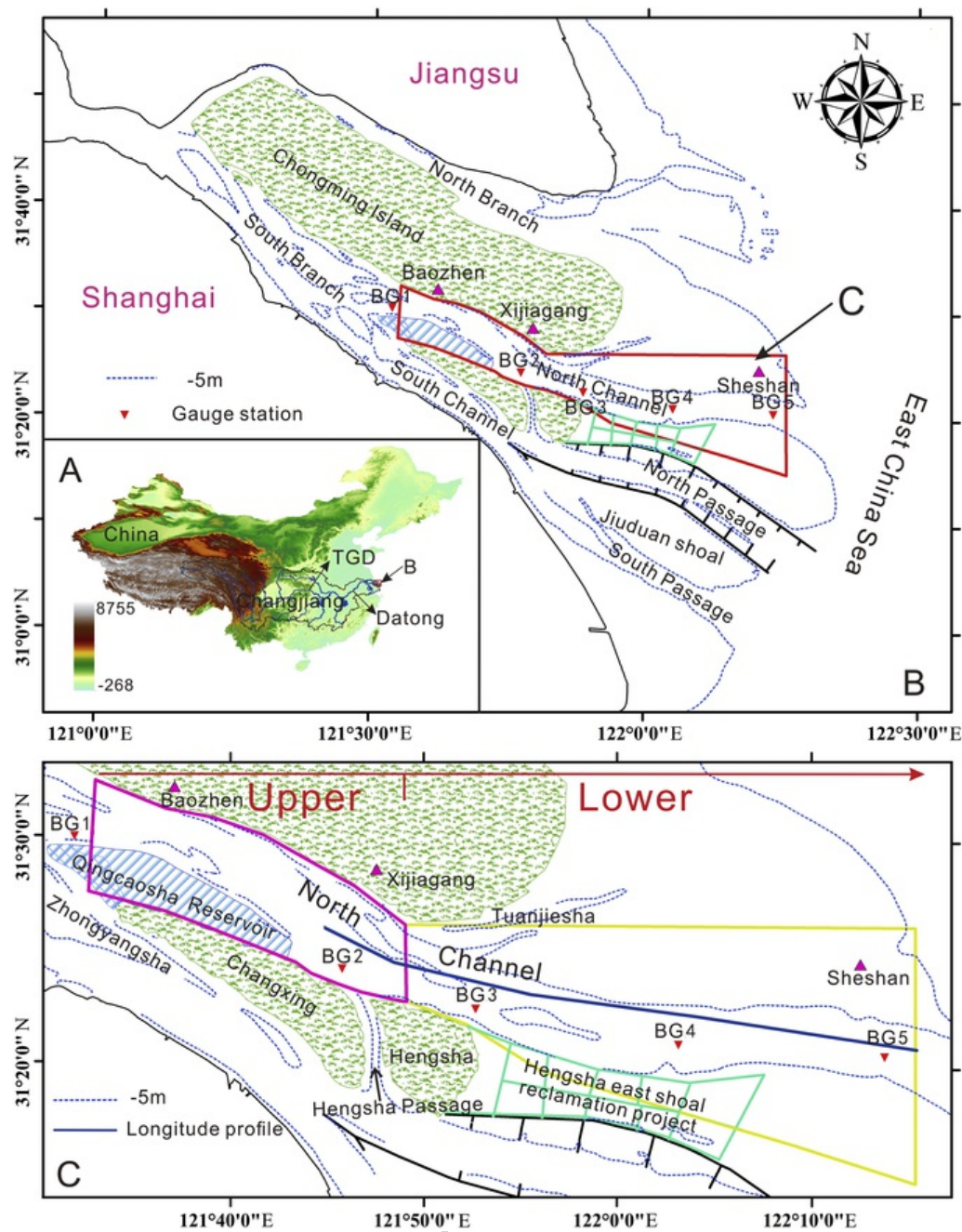
Fig. 1 Map showing the study area, with A) the Changjiang River's location in relation to China and the location of the Three Gorges Dam and Datong station; B) Changjiang Estuary; C) North Channel.

alt-text: Fig. 1

NC, the largest bifurcated estuary of the Changjiang River, was in fact in a natural state over a long period of time until the 2003 closing of the TGD. Study of the NC's evolution have detected the relative dominance of natural forcings, such as fluvial discharge, tidal discharge and asymmetry between the flood and ebb tides. Moreover, around 50% of the riverine water and sediment discharge flows into the East China Sea through NC, bathymetric variation of the NC therefore

can effectively reflect the influence of TGD induced water and sediment variations on estuarine morphology. Further, the NC suffered local human interferences since 2007, such as Qingcaosha Reservoir regulation and land reclamation, which will further alter the estuarine morphology. Accordingly, NC is a perfect place to study the natural processes governing estuarine evolution as well as the effects of the historically recent human impacts. Besides, previous studies have mainly focused on the decadal morphological evolution of the Changjiang Estuary since the 1950s (e.g. Luan et al., 2017; Dai et al., 2014), however, little work has been conducted at centennial scale. The current study therefore aims to assess the long-term bathymetric variations of the NC during the period 1880–2013 to address this research gap and add to the knowledge base on the geomorphologic system of the Changjiang Estuary.

2.2 Geographical setting

The Changjiang Estuary, with a length of 120 km and a width of 90 km at its outer limit, has developed a three-order bifurcation and four-outlet configuration over the past millennia (Chen et al., 1979). Specifically, the first order bifurcation consists of the South and North Branch, separated by Chongming Island. The South Branch is further divided into the South and North Channel by Changxing and Hengsha islands, serving as the second order bifurcation. The South Channel thereafter is followed by the South and North Passage as the last bifurcation, separated by the Jiuduansha Shoal (Fig. 1B). Currently, the North Branch, North Channel, North Passage and South Passage are the four main entrances open to the East China Sea.

As the north distributary of the second order bifurcation, the NC is almost purely natural in its conditions, with the least disturbance from human influence. The channel can be further divided into two sub-areas: the upper reach from approximately 6 km above Baozhen to around 5 km below Xijiagang, namely, the inner side of the mouth bar, and the lower reach around 5 km below Xijiagang to 5 km below Sheshan, the mouth bar and its outer side area (Fig. 1C). Hengsha Passage, located between Changxing and Hengsha islands, is a typical ebb channel that connects the NC with the North Passage.

3.3 Data and methods

3.1.3.1 Data acquisition

The bathymetric data of the NC, in uneven intervals over the period 1880–2013, were collected from different sources, with the map from 1880 to 1997 monitored by Maritime Survey Bureau of Shanghai (MSBS) and the chart since 2002 provided by the Changjiang Estuary Waterway Administration Bureau (CJWAB) (Table 1). Dual-frequency echo sounders was used for depth information, with a vertical error of 0.1 m. Theodolite and GPS devices were respectively adopted over 1880–1987 (with an error of 50 m) and 1988–2013 (with an error of 1 m) for positioning. The map scale ranged from 1:50,000 to 1: 10,000 with a data density of 8–20 points per km². Monthly river discharge at Hankou (1865–2013), monthly river discharge (1950–2013) and sediment load (1954–2013) at Datong station, the most downstream hydrologic station in the Changjiang River, were obtained from the Changjiang Water Resources Commission. In addition, tidal flow and suspended sediment concentration (SSC) measurements were carried out during spring tide at locations BG1 (2006.8, 2010.8, 2011.8, 2015.7) and BG2 (2012.8, 2015.7), respectively (Fig. 1C). Besides, a thorough survey was conducted along the NC in August, 2012, when a series of parameters, including water discharge and SSC are obtained at BG2–5 (Fig. 1C). It needs to be mentioned that BG1 was initially set around 3 km upstream of its present location in 2006, but moved to its current location in 2010. In view of the similar hydrodynamic conditions between the two locations, the measurements in 2006, 2010, 2011 and 2015 can be classified into one group to demonstrate the flow and sediment features around the NC head.

Table 1 Details about the bathymetric data of the North Channel, Changjiang Estuary.

alt-text: Table 1

Survey date	Scale	Data sources
1880;1906;1920;1959;1965;1971;1973; 1980; 1982; 1989; 1994; 1997	1:50,000	MSBS
2002; 2004	1:25,000	CJWAB
2007; 2009; 2010; 2012; 2013	1:10,000	CJWAB

Note: MSBS: Maritime Survey Bureau of Shanghai (MSBS), Ministry of Communications of China.
　　　CJWAB: Changjiang Estuary Waterway Administration Bureau (CJWAB), Ministry of Transportation of China

3.2.3.2 Data processing and analysis

The morphodynamic processes of the NC during the period 1880–2013 are explored based on the bathymetric data through a series of analyses, including morphological changes, water depth and channel volume variations (van der Wal et al., 2002; Blott et al., 2006). The 19 charts were firstly transformed into depth points relative to Beijing 54 coordinates and calibrated into 'Wusong Datum' using ArcGIS. Thereafter, the vector bathymetric point data from each survey were gridded using the Kriging scheme into 50 × 50 m resolution to produce a digital elevation model (DEM) (Burrough and McDonnell, 1998). Deposition and erosion patterns were then obtained by subtracting the two subsequent morphological surveys.

Empirical Orthogonal Functions (EOF) provide an efficient means of extracting the dominant modes of variability from a given DEM data set (Dai et al., 2015). This was achieved here by isolating the temporal and spatial dependence of the data through a series of linear combination functions in time and space (Miller and Dean, 2007):

$$y(x,t) = \sum_{k=1}^{n} a_k c_k(t) e_k(x) \tag{1}$$

Where $e_k(x)$ and $c_k(t)$ are referred to as the spatial and temporal eigenfunctions, respectively. n is the lesser of n_x and n_t, the number of spatial and temporal samples. a_k is a normalizing factor, given by:

$$a_k = \sqrt{\lambda_k n_x n_t} \tag{2}$$

Where λ_k is the eigenvalue of the kth eigenfunction.

Mathematically, the spatial eigenfunction $e_k(x)$ and eigenvalues λ_k can be obtained through the Lagrange multiplier approach.

$$A e_k(x) = \lambda_k e_k(x) \tag{3}$$

Where A is a measure of the spatial covariability of the data, which can be taken as the correlation or sum of squares and cross products matrix

$$A = \frac{1}{n_x n_t} \left(YY^T \right) [n_x, n_t]$$

(4)

Where Y is made up of the individual elements of $y(x, t)$ and Y^T is the transpose of Y.

The temporal eigenfunctions can be calculated directly through an analogous procedure. Thus the relative contribution of mode k to the total variability can be calculated according to:

$$p_k = \left(\frac{\lambda_k}{\sum\limits_{k=1}^{K} \lambda_k} \right) \times 100$$

(5)

Monthly water discharge at Datong from 1865 to 1949 were reconstructed through a regression method (Yang et al., 2010). Specifically, for each month of the year, linear equations between the discharge at Hankou and Datong are established based on observations during the period 1950–2002 (Supplementary Fig. S1), excluding the effects of the TGD. Then the monthly discharge at Datong for the missing months (1865–1949) can be calculated using the regression equation with the corresponding observed discharge at Hankou. Monthly sediment discharge at Datong from 1865 to 1953 were reconstructed using a similar approach. Firstly, for each month of the year, power-law relationships to relate water sediment to water discharge were established for Datong station based on observations made during 1955–1968 (Supplementary Fig. S2), when the effects of human disturbance were nearly negligible (Wang et al., 2008b). The unknown monthly sediment loads from 1865 to 1953 were thereafter estimated through the rating curves and the corresponding monthly discharge. Thus the yearly water and sediment discharge can be extended to 1865–2013 by summing the monthly value.

At each hydrographic station, the coefficient of flow/sediment dominance was calculated (Simmons, 1955) using:

$$A = \left(\frac{Q_e}{Q_e + Q_f} \right) \times 100\%$$

(6)

Where A is the coefficient of flow/sediment dominance, Q_e is the cross sectional averaged ebb flow/sediment rate, Q_f is the cross sectional averaged flood flow/sediment rate. When $A > 50\%$, the flow/sediment is ebb dominant, otherwise, it is flood dominant.

4.4 Results

4.1 4.1 Morphological configuration of the North Channel

Over the study period 1880–2013, the NC retains essentially the same configuration, with the inner side of the mouth bar exhibiting a 112° clockwise configuration, consistent with the main direction of the ebb tide and the mouth bar and its outer side area, which indicates an angle of 108° clockwise. Specifically, its morphological evolution exhibits variant characteristics in different periods. In 1880, the NC has a single morphological state, with scattered sandbars located in the upper reach around Qincaosha shoal and a large cluster of shoals less than −5 m around the mouth bar area (Fig. 2A). Thereafter, the previously isolated sandbars gradually grow larger while the lower reach formed Chongming Shoal and Hengsha Shoal in 1906 due to continuous sediment accumulation from upstream (Chen et al., 2007). In the meantime, sandbars (higher than −2 m) occur around Chongming and Hengsha Islands. Hengsha Passage appears in the south of the NC, which connects NC with the North Passage (Fig. 2B). Then in 1920, sandbars in the upper reach further developed and adopted a fist-shape with fingers pointing downstream, thus producing three flood tidal channels under the dominance of tidal flood current (Fig. 2C). In 1959, the irregular sandbars in the deep channel suddenly become smooth after the catastrophic 1954 flood (Fig. 2D). In the following years, NC changes repeatedly, switching from a condition with sandbars aggregating and flood tidal channel developing (Fig. 2E-F, H-I, K-L, N-S) to a configuration in which the channel is completely smooth (Fig. 2G, J, M) following the occurrence of extreme floods.
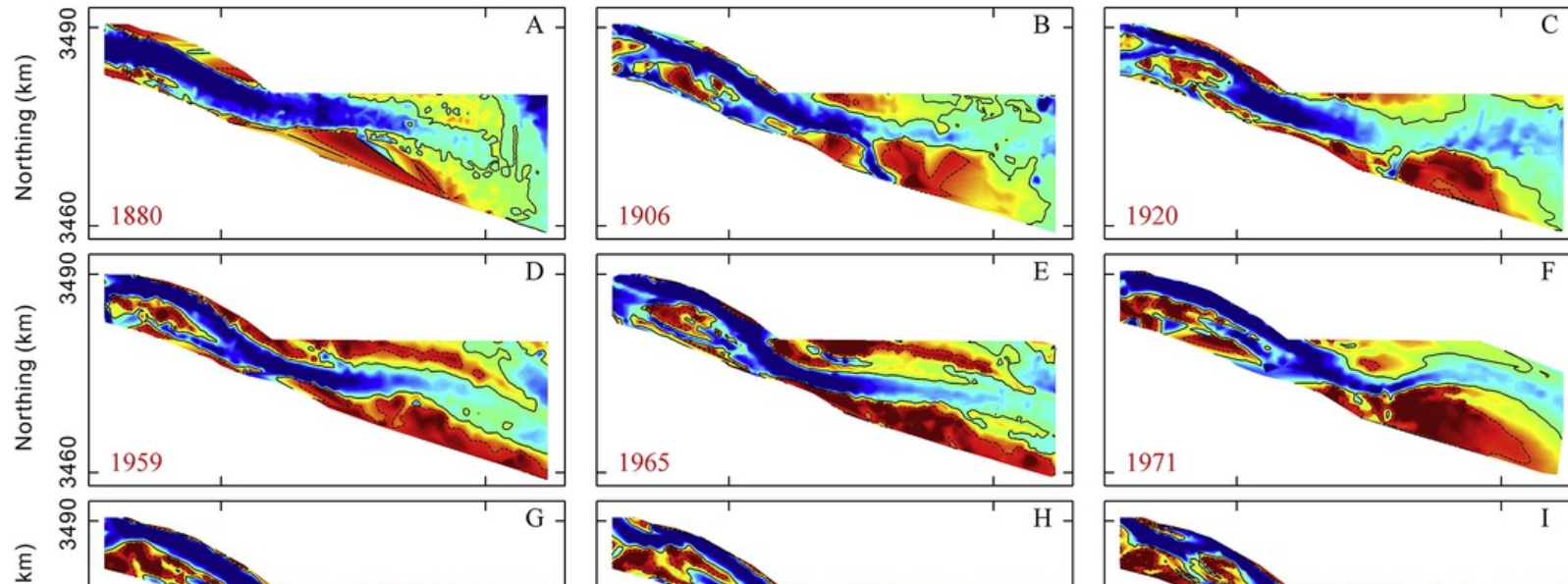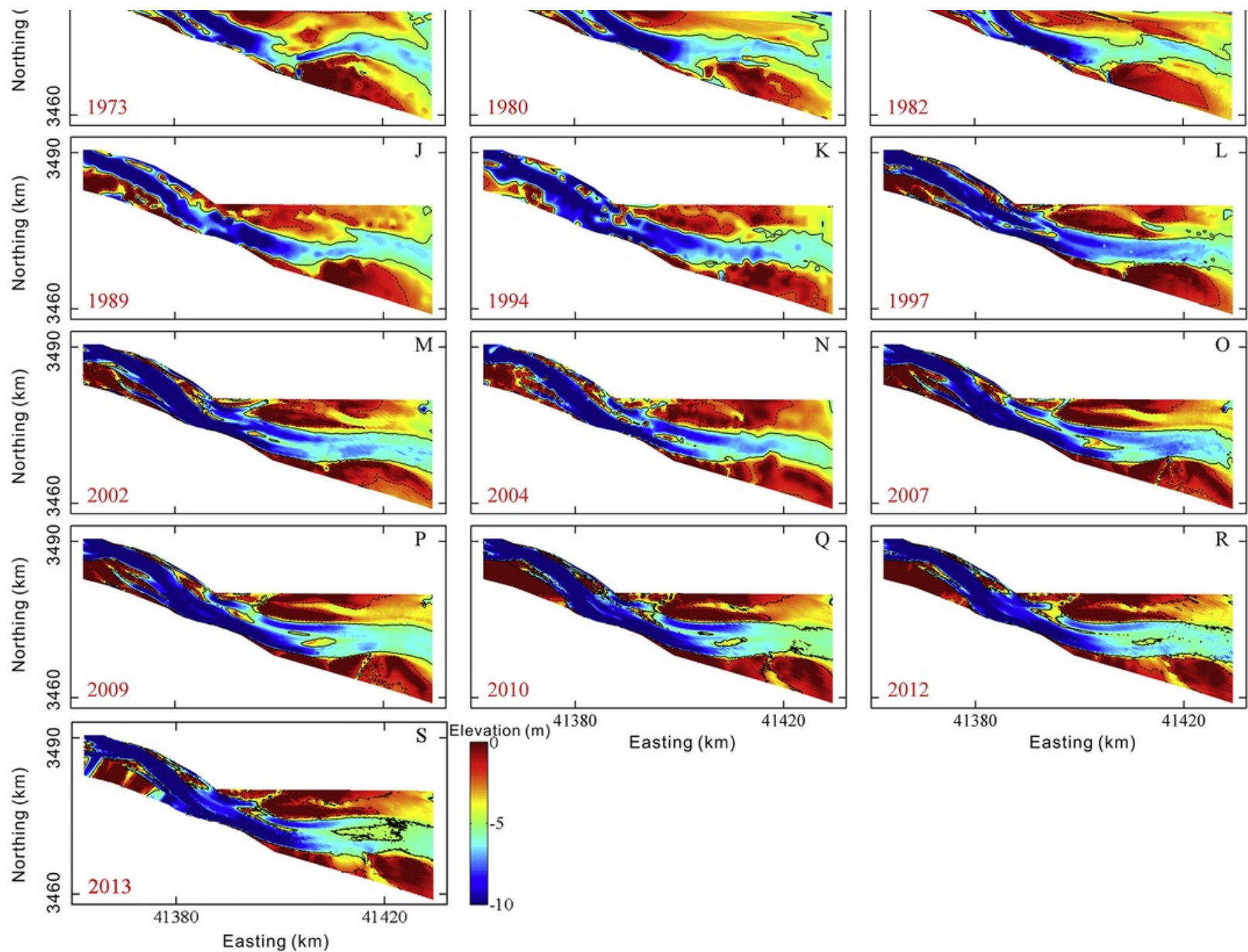
Fig. 2 Bathymetric maps of the North Channel over the period 1880 to 2013.

alt-text: Fig. 2

4.2.4.2 Variations of the mean water depth and volumes along the North Channel

Mean water depth over the NC has a value of around 5 m over the past 130 years, with a deeper depth of 6.9 m in the upper reach and a shallow depth of 4.2 m in the lower reach (Fig. 3). Water depths of both the entire reach and lower reach have exhibited a statistically significant downward trend during the period 1880 to 2013 ($p < 0.001$), in spite of a high volatility during the period 1982–2012 (Fig. 3B-C). Meanwhile, no significant temporal trend is detected in the water depth of the upper reach (Fig. 3A).
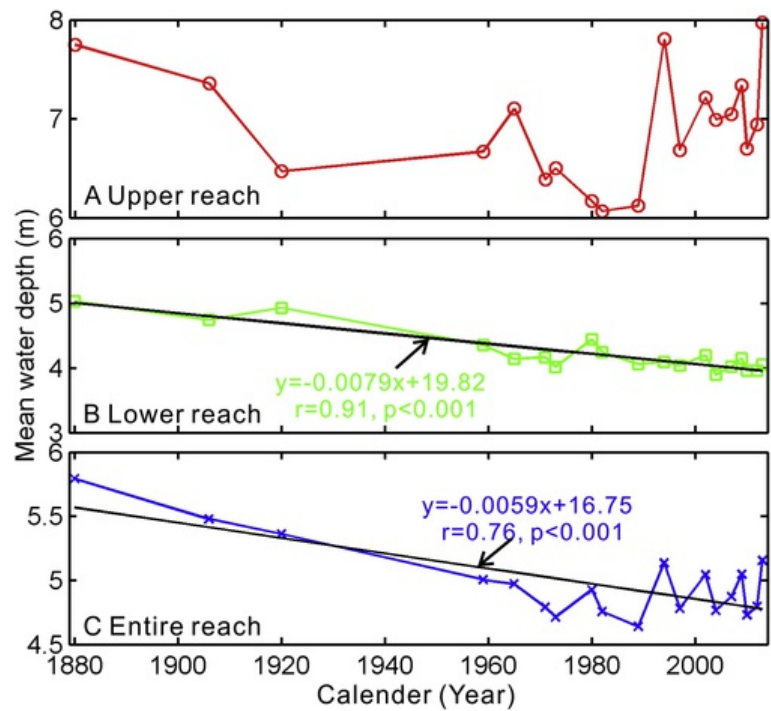
Fig. 3 Yearly variations of mean water depth, for A) upper reach; B) lower reach; C) the entire reach.

alt-text: Fig. 3

The channel volume below 0 m shows similar trends as the water depth. Both the entire reach and the lower reach indicate a smaller storage below 0 m with jumpy volume variations during the period 1980 and 2013 when the fluctuation is as high as $0.2 \times 10^9 \, m^3$ (Fig. 4B-C). Channel volume below −5 m, however, exhibits different processes, with the upper, lower and entire reach all indicating insignificant variations (Fig. 5). It needs to be stressed that the volume below −5 m increases significantly by $0.5 \times 10^9 \, m^3$ during 1994—2013 for the entire reach, which is mainly contributed by the upper reach (Fig. 5A–B).
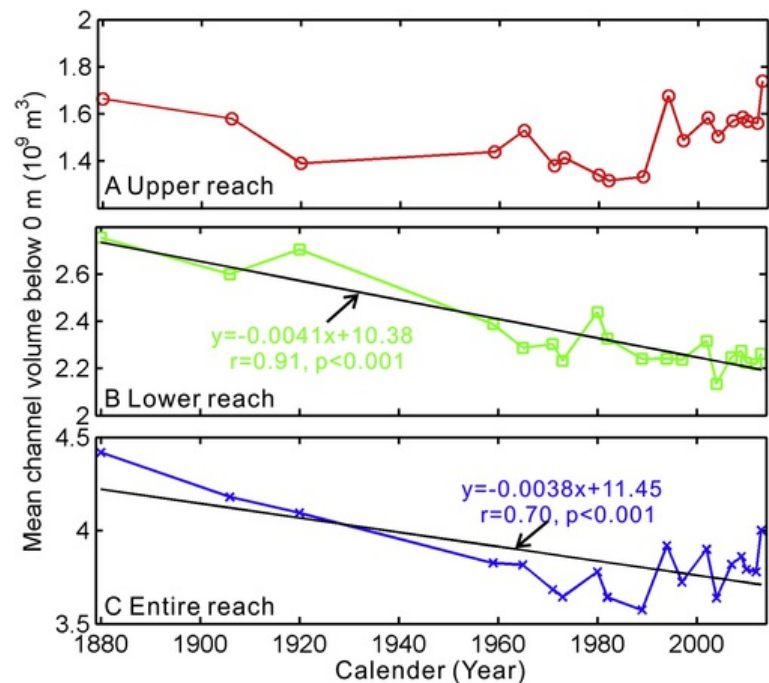
Fig. 4 Yearly variation of channel volume below 0 m isobath, with A) the upper reach; B) the lower reach; C) the entire reach.
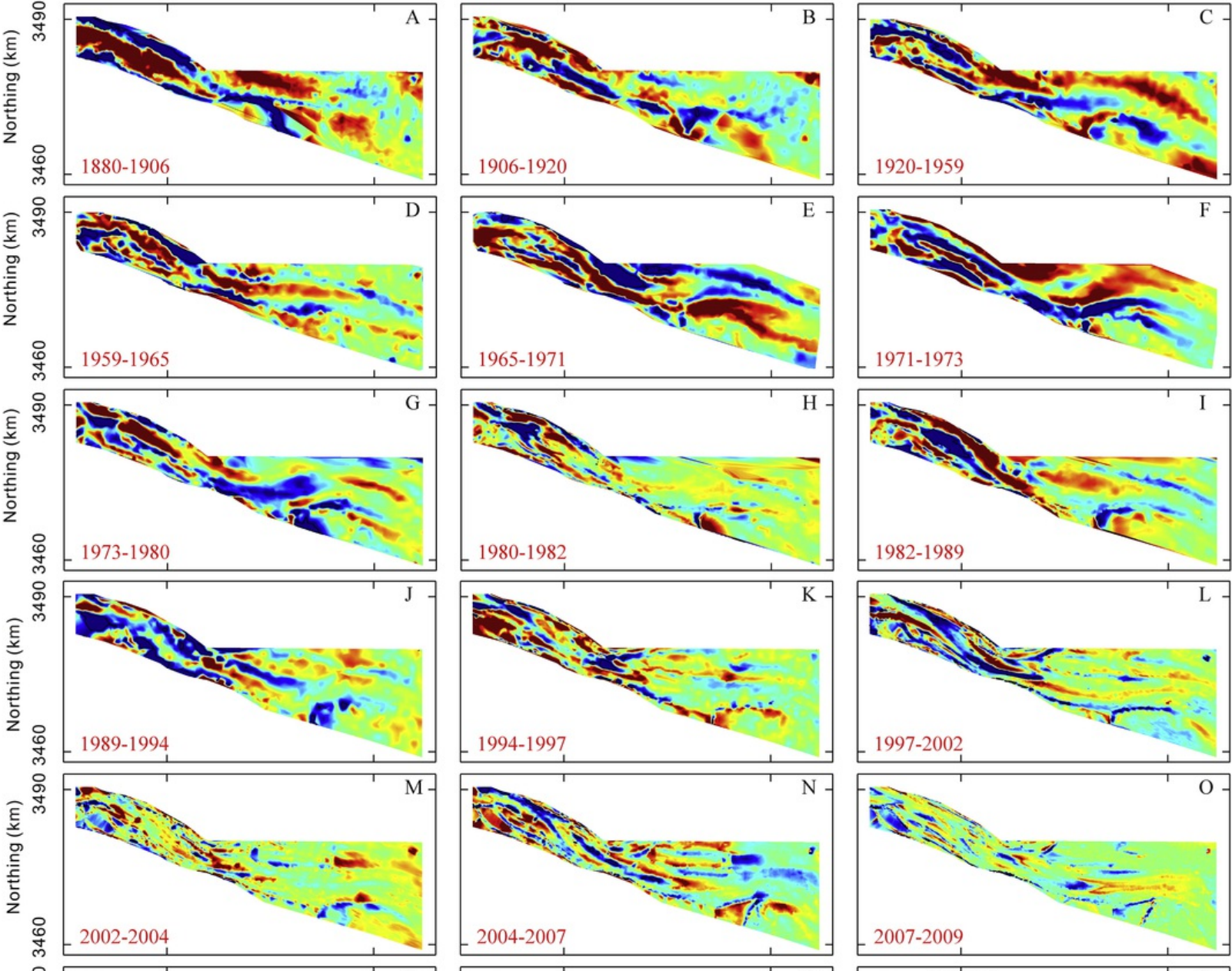
alt-text: Fig. 4

4.3. 4.3 Bathymetric changes between 1880 and 2013

North Channel exhibits a relatively moderate erosion/deposition pattern during 1880 to 2013, with yearly elevation variations ranging between -2 m and 2 m (Fig. 6). Specifically, the channel is in a net depositional state from 1880 to 1989, followed by overlays of slight erosion and slight deposition from 1994 to 2013. Such variations are in accordance with the changes of channel volume below the 0 m isobath (Fig. 4C).
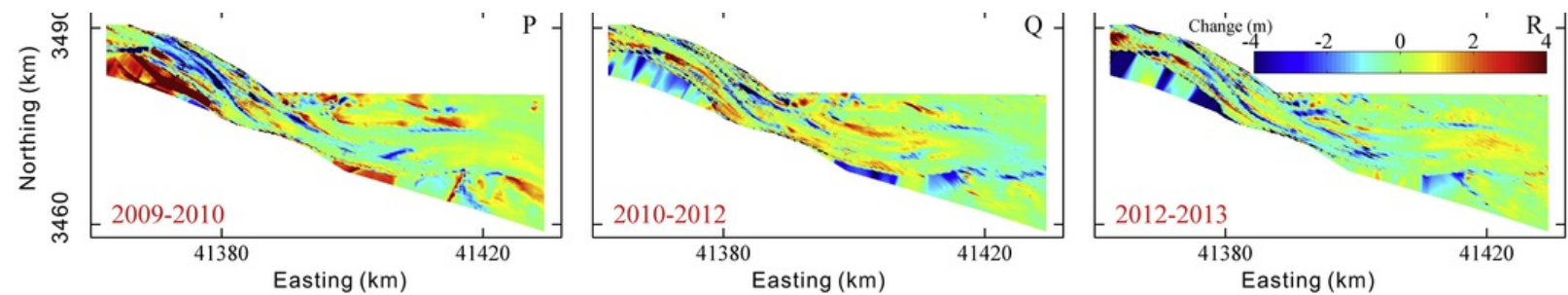
Fig. 6 Yearly erosion/deposition patterns of the North Channel at un-uniform intervals from 1880 to 2013.

alt-text: Fig. 6

However, the erosion/deposition pattern of the NC indicates significant spatial differences. While the lower reach from Xijiagang to the channel mouth remains on a state of continuous deposition of 0.3 m per year, dramatic erosion is detected in the deep channel of the upper reach, which exhibits observable erosion as deep as 4 m during 1880–1906, 1920–1959, 1971–1973, 1982–1989, 1997–2002 and 2004–2007 (Fig. 6A, C, F, I, L, N). Besides, deposition frequently occurs in the middle zone where the upper and lower reach are connected. A series of time intervals, such as 1906–1920, 1959–1965, 1965–1971, 1971–1973, 1982–1989 and 2004–2007, all exhibit accretion around the middle zone (Fig. 6B, D, E, F, I, N). The spatial morphological evolution can be also reflected by the channel thalweg, which has an observable bulge in the zone 10–20 km away from the beginning point, where the large scale mouth bar is located (Fig. 7). The outer side of the mouth bar, approximately 35–40 km away from the beginning point, indicates observable deposition since 2007, with an annual accumulation of 0.2 m (Fig. 7D).
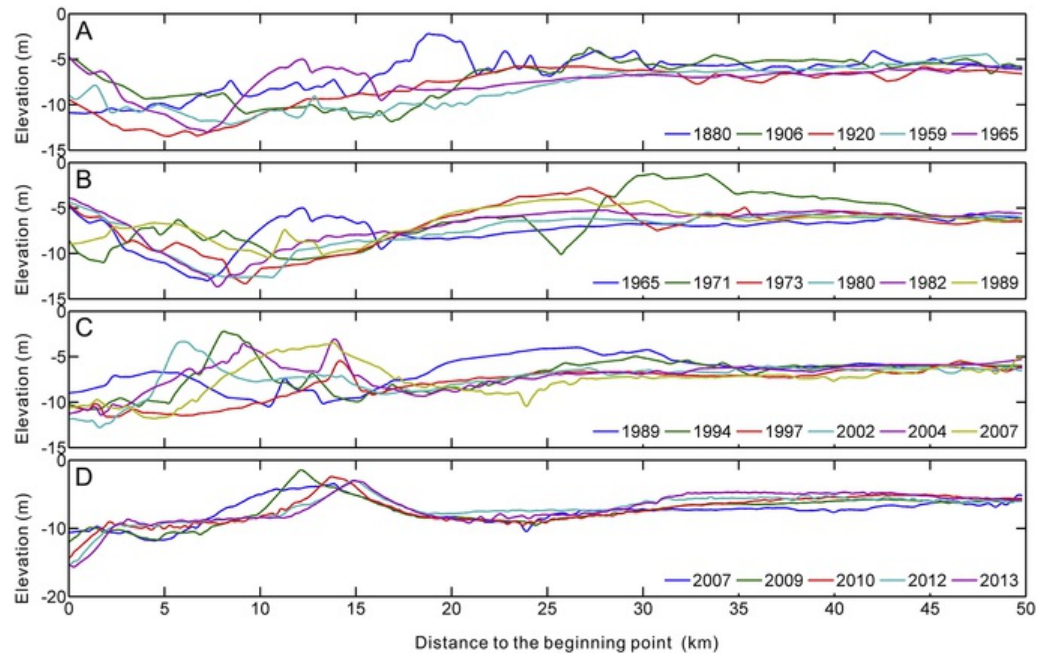

Fig. 7 Temporal bathymetric variations of the North Channel from 1842 to 2013. The location of the longitudinal section is shown in Fig. 1.

alt-text: Fig. 7

4.4. Erosion/accretion patterns

The EOF decomposition of the bathymetric survey in NC produces two distinct modes, which take up over 75% of the total variability (Fig. 8). In view of the small contribution of the remaining EOF modes, only the first two modes are considered afterwards to characterize the NC's morphological evolution during 1880–2013.
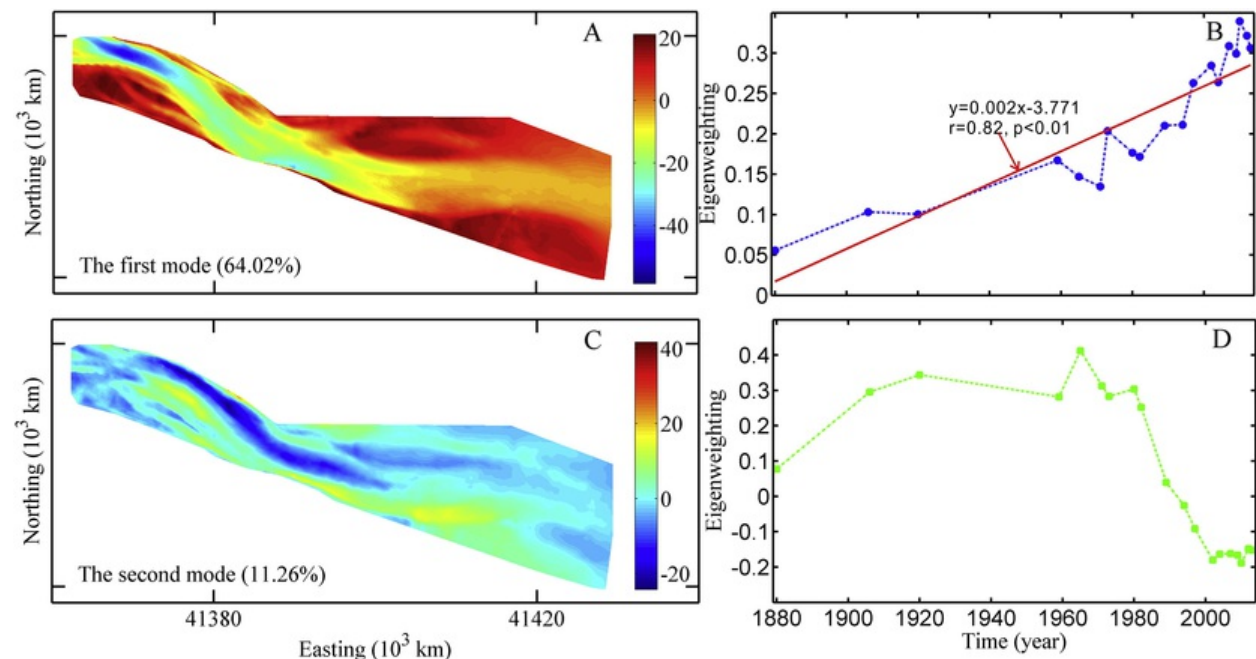
Fig. 8 EOF analysis of the bathymetric records in the North Channel, with (A, C) two distinct modes of bathymetric variability and their (B, D) eigenweighting vectors.

alt-text: Fig. 8

As expected, the first mode explains the majority of the variability (over 64%). The spatial eigenfunction indicates positive covariance in most parts of the shoal and channel, except the deep channel adjacent to the entrance of the upper reach (Fig. 8A). The associated temporal variability exhibits a significant upward trend with $p < 0.01$ (Fig. 8B), which mainly describes the continuous deposition along the lower reach of NC.

The second mode represents ~~more than~~ ≥ 11% of the overall variability in the DEM data. The spatial covariability shows a large scale of negative values along the NC, especially for the deep channel of the upper reach, where the negative value reaches −20 m (Fig. 8C). Meanwhile, the temporal vectors show a shift from positive to negative values around 1983 (Fig. 8D). The increasing trend in temporal eigenweighting vectors during 1880–1982, coupled with the spatial eigenfunction features, indicate that the deep channel of the upper reach is in an erosional state. Such a phenomenon coincides well with the channel capacity variation below the −5 isobath of the upper reach (Fig. 9). Accordingly, the second mode mainly explains the morphological evolution of the deep channel below the −5 m isobath of the upper reach, which exhibits an overall trend of erosion.
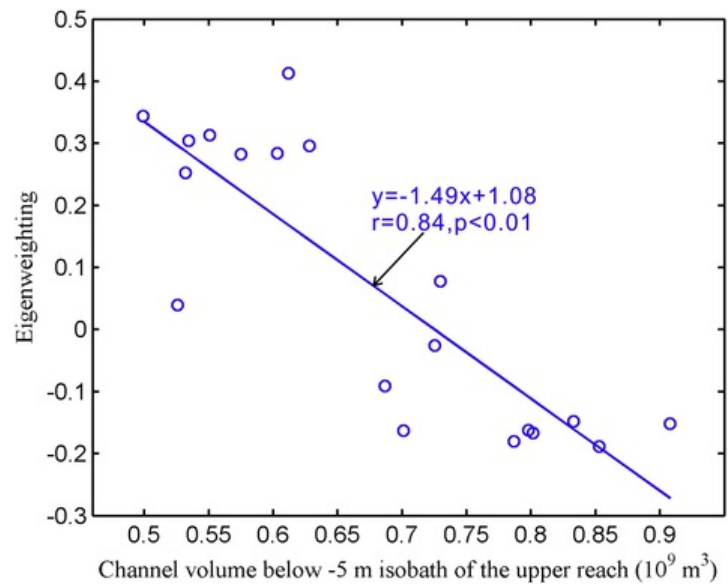
Fig. 9 The relationship between eigenweighting of the second EOF mode and channel volume below the -5 m isobath of the upper reach

alt-text: Fig. 9

5.5 Discussion

In view of its geographical location, morphodynamic processes of the NC are affected by both riverine and coastal sediments, local hydrodynamics, and extreme climate events. Their potential influences are further discussed in this section.

5.1.5.1 Sediment availability from upstream

The erosion/accretion pattern along the NC depends on the sediment availability and transport from the upland river system. Yearly riverine sediment from the Changjiang River into the estuary shows a notable step decrease during the period 1865–2013. Specifically, the yearly suspended sediment discharge is relatively stable from 1865 to 1968, with a mean value of 504×10^6 t/yr, which decreases slightly to 427×10^6 t/yr during 1969–1990 and further to 326×10^6 t/yr during 1991–2002, but sharply to 143×10^6 t/yr during 2003–2013 (Fig. 10A). Such trends can be explained by dam constructions and soil conservation in the upstream basin, especially the construction of the TGD in 2003 (Chen et al., 2010; Dai et al., 2016a, 2016b).
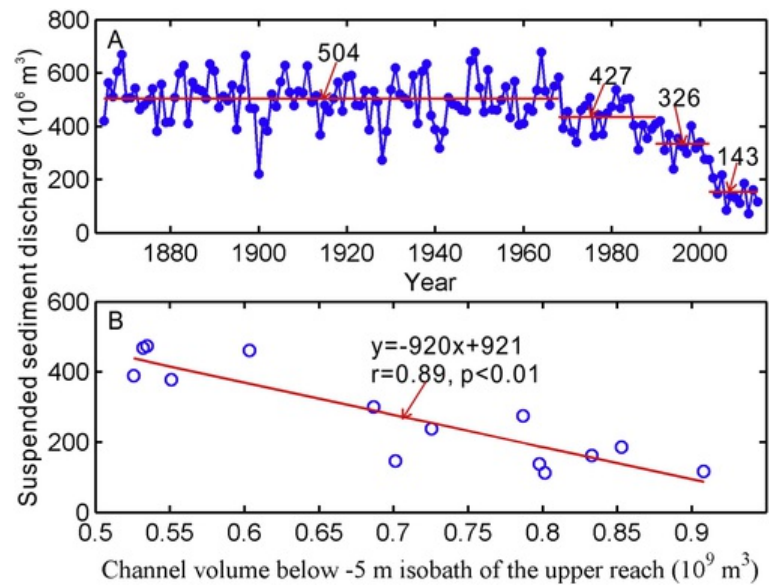
Fig. 10 A) Yearly suspended sediment discharge (SSD) into the Changjiang Estuary; B) the relationship between SSD and channel volume of the upper reach.

alt-text: Fig. 10

The decrease in riverine sediment is apparently inconsistent with the decreases in channel volume below the 0 m isobaths (Fig. 4C), especially to that of the lower reach (Fig. 4B), which indicates that there is more sediment entering into the NC. Therefore, the decreasing sediment supply from upstream has no apparent significant contribution to the channel volume variation of the entire reach. On the contrary, the upper reach of NC exhibits a statistically significant increase in channel volume below the − 5 m isobaths coinciding with the recent dramatic decrease in riverine sediment availability during 1970−2013 (Fig. 10B). More specifically, the average yearly channel volume increases suddenly from 0.68×10^9 m^3 in the 1990s to 0.82×10^9 m^3 in the post-TGD period, while the riverine sediment load decreases by over 50%, suggesting that the morphology of the upper reach is dominated by the fluvial sediment from the upland Changjiang River. This coincides well with the SSC variation along the upper reach, where the vertical averaged SSC and vertical averaged maximum SSC respectively reduce by 0.35 kg/m^3 and 0.55 kg/m^3 during flood tides from 2006 to 2015 (Fig. 11). The decreasing riverine sediment only directly affects the area around the inner side of the mouth bar, which possibly results from the buffering effect of mouth bar and marine sediment compensation (Luan et al., 2016). The second mode of the EOF function describes a similar phenomenon, namely that the significant increase in channel volume below − 5 m isobaths of the upper reach is attributed to TGD-induced riverine sediment reduction (Fig. 9). As for the morphology of the lower reach, which, however, is likely dominated by other drivers.
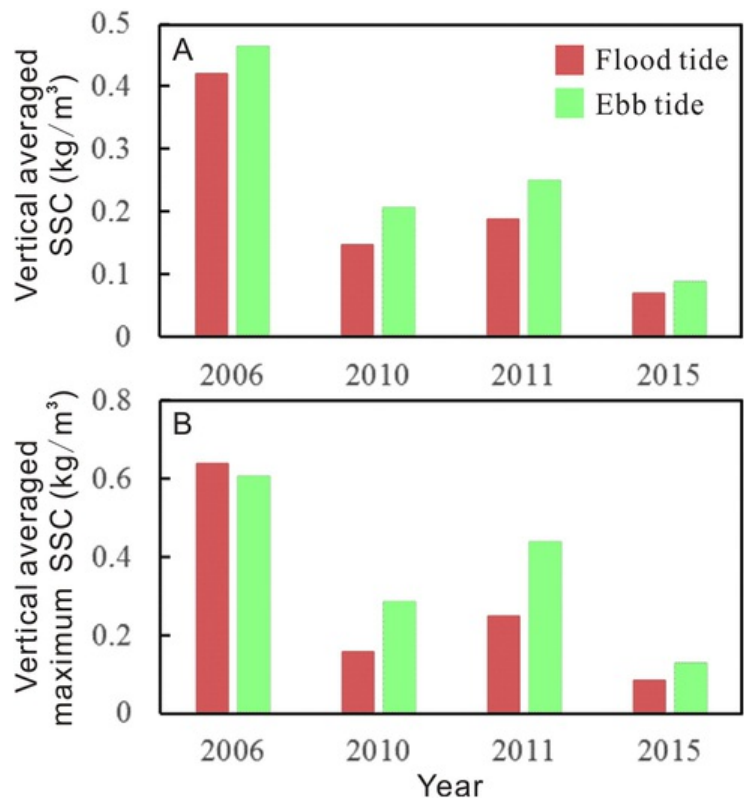
Fig. 11 A) Vertical averaged SSC during flood and ebb tides at the BG1 station; B) Vertical averaged maximum SSC during flood and ebb tides at the BG1 station.

alt-text: Fig. 11

~~5.2.~~5.2 Local influences

The mouth bar area is a natural barrier with intensive interaction between the marine and fluvial zones, where the fresh and salt water mixing is favorable for suspended sediment deposition owing to flocculation (Liu et al., 2016), gravitation circulation (Uncles and Stephens, 1997) and tidal pumping (Mitchell et al., 2003). As an example, the SSC distribution characteristics along the NC in August 2012 are described in Fig. 12A-D. It is observable that the average SSC during the flood and ebb tide respectively show maximum values at BG4 and BG5, in particular, around the bottom surface, which increase by 4.07 kg/m^3 and 3.05 kg/m^3 in comparison with that of the upper NC reach at BG2. The area with high SSC coincides well with the high deposition zone as well as the turbidity maximum zone of the NC. Meanwhile, the coefficient of dominant flow decreases gradually along the NC (Fig. 12E-H), especially for the area around the channel bed, where the coefficient of dominant flow declines from 89% in the upper reach at BG2 to 52% around the channel mouth at BG5. As a result of tidal asymmetry (Dronkers, 1986), the sediment dominance switches from ebb dominance to flood dominance in the lower reach at BG4 (Fig. 12I-L), indicating the occurrence of mouth deposition.
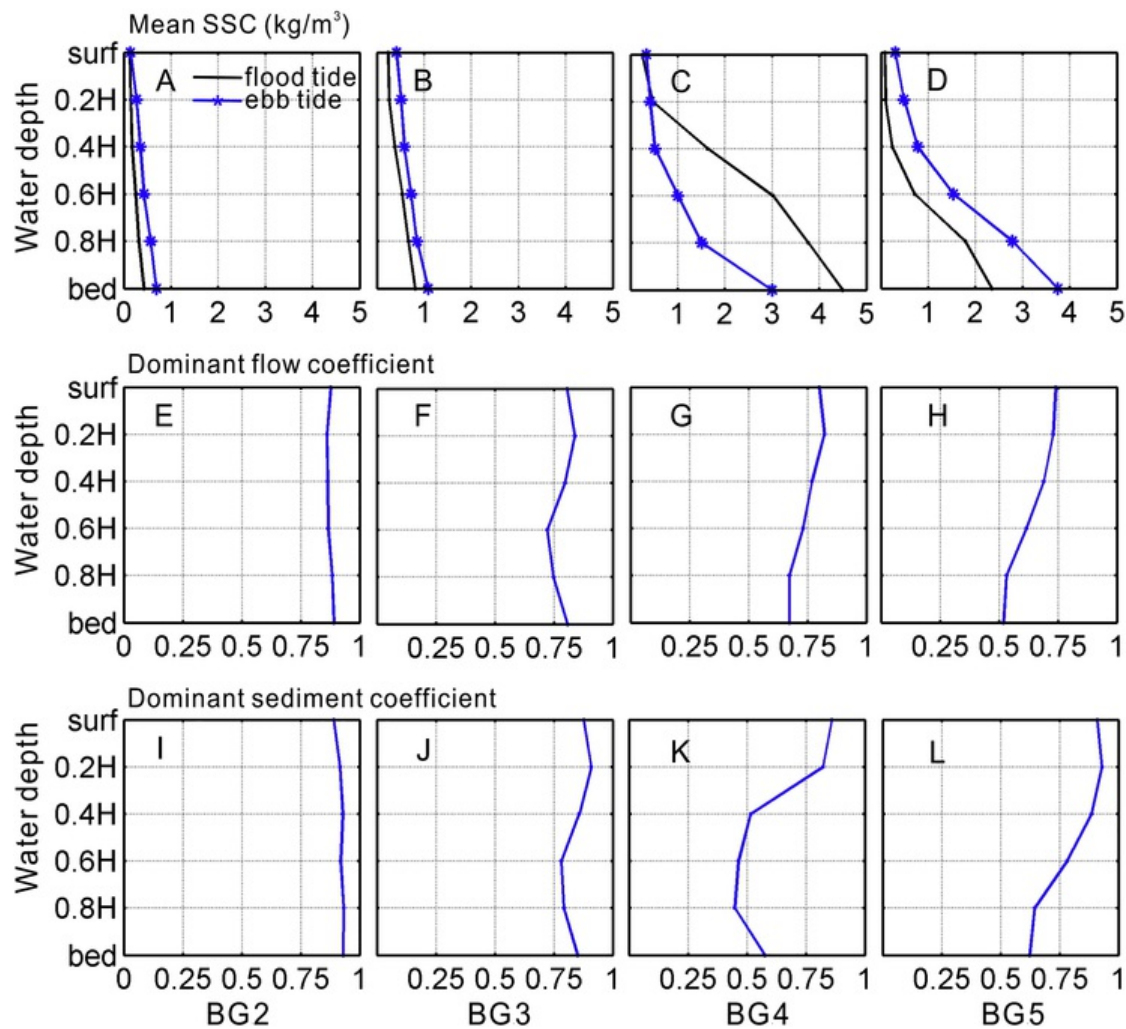
Fig. 12 A–D) Averaged SSC; E–H) coefficient of dominant flow; I–L) coefficient of dominant sediment along the NC in August 2012.

alt-text: Fig. 12

Human interference along the NC mainly consists of the Qingcaosha Reservoir construction around the channel head (2007–2011), and tidal flat reclamation in the lower reach (2003–2015) (Fig. 1C). Along with the seaward extension of the Qingcaosha Reservoir, the upper reach of NC is narrowing gradually, which increases the dominant current/sediment from 50- to 55% in 2006 to around 90% in 2015 (Fig. 13A). In the meantime, local SSC decreases from 0.42 kg/m³ to 0.07 kg/m³ (Fig.11A), which therefore results in strong erosion along the frontal river bed of the reservoir (Sheng et al., 2017). The significant erosion along the deep channel of the upper reach has also been reflected by the second mode of the EOF function (Fig. 9).
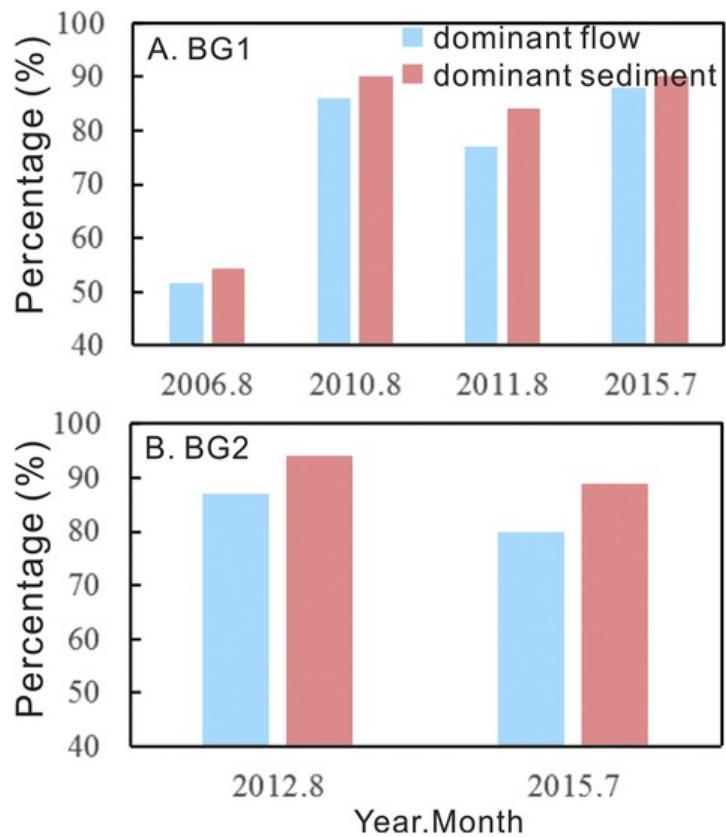
Fig. 13 A) The coefficient of dominant flow and sediment during the flood season at the BG1 station; B) the coefficient of dominant flow and sediment during the flood season at the BG2 station.

alt-text: Fig. 13

It needs to be stressed that the riverine discharge is characterized by a 'no flood in flood season' management regime since the construction of the TGD (Mei et al., 2016), which reduces the occurrence of high flow discharge and thus in turn enhances the flood-tide force along the estuary (Swenson et al., 2005). Meanwhile, the reach around the mouth bar exhibits a width contraction of 0.9 km owing to the tidal flat reclamation project during 2003–2015 (Fig. 1C), which results in the flood-tide being further strengthened. Thus a tendency can also be manifested by the variation in the coefficient of flow and sediment dominance around the lower reach, which respectively decreased by approximately 8% and 5% from 2012 to 2015 (Fig. 13B). The increasing flood-tide force following the TGD-induced riverine discharge decrease and land reclamation induced lower reach narrowing is likely resulting in net sediment import (Chu et al., 2015) and large scale accretion along the lower reach, which has been clearly demonstrated in the channel thalweg response along the lower reach during 2007–2013 (Fig. 7D) and the first mode of the EOF function (Fig. 8A).

5.3.5.3 Episodic extreme floods

Coastal areas are prone to storms and extreme floods (Fig. 14A), which may have significant influences on the estuarine and delta morphological evolution (Törnqvist et al., 2006; Luan et al., 2016). Naturally, the geomorphology of the NC is characterized by scattered sandbars and a narrow and curving deep channel along the upper reach (Fig. 2C, I). Following the extreme flood of 1954, 1983 and 1998, the NC becomes smoother and wider immediately (Fig. 2D, J, M), suggesting extensive geomorphic variations. Thereafter the channel gradually readjusts to its pre-flood morphology during years of low peak flow with scattered sandbars developing and channel narrowing and curving (Fig. 2E, N). Evaluation of the NC morphology suggests that the NC is in an infinite loop between flood and reset (Fig. 14B): the channel changes markedly during each extreme flood with rapid and extensive morphological variations, thereafter, it returns to its original state by self-adjusting over decadal timescales. The cycle of NC reset followed by channel smoothing and expansion is a typical episodic disequilibrium (Nanson and Erskine, 1988).
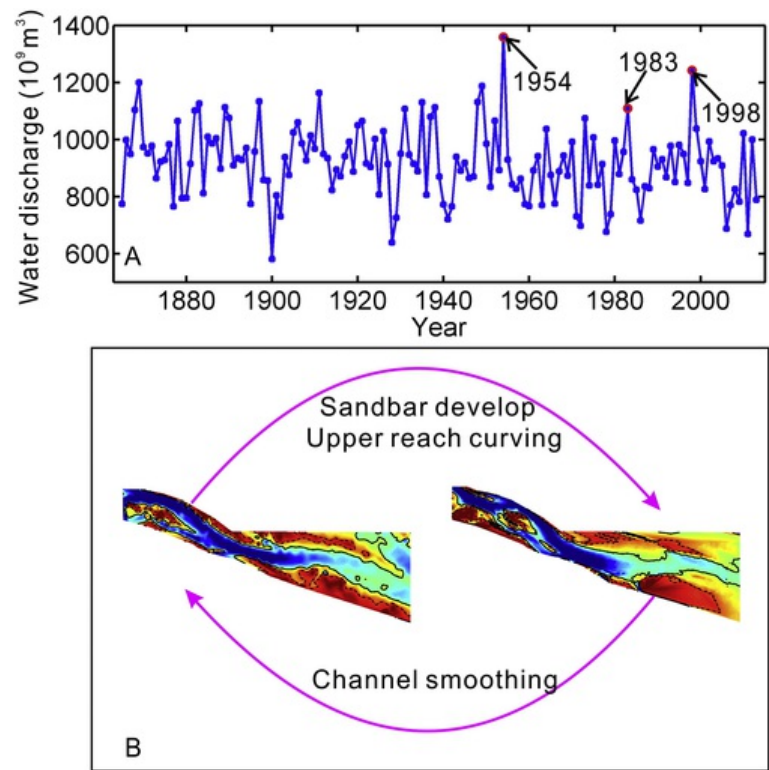
Fig. 14 A) Yearly water discharge into the Changjiang Estuary with recent extreme floods highlighted by the red cycles; B) Cyclic evolution of the North Channel relative to the extreme floods (For interpretation of the references to colour in this figure legend, the reader is referred to the web version of this article.)

alt-text: Fig. 14

6.6 Conclusions

Estuaries, located at the transition zone between rivers and the open sea, are under the influence of more frequent extreme climate events and intensified human activities. In this study, North Channel, the largest bifurcated estuary of the Changjiang River, is used as a case study to explore estuarine bathymetric variations in response to natural and human interferences, at centennial scale for the period 1880–2013. The main conclusions are as follows:

1). Channel capacity of the entire NC has been decreasing during the period 1880–2013. Although the upper reach (inner side of the mouth bar) has exhibited significant erosion in channel volume below – 5 m during 1970–2013, this is overruled by the dramatic deposition in the lower reach (mouth bar area and its outer side).

2) Bathymetric variations of the NC are dominated by both the upstream sediment availability and the relative strength between the river discharge and local tidal force. While the recent period, erosion in the upper reach is attributed to riverine sediment declining, particularly since 2003 when the TGD was established. In contrast, deposition along the lower reach since 2003 can be explained by landward sediment transport due to the flood-tide force increasing under the combined effects of a decrease in TGD-induced river discharge and land reclamation induced lower reach narrowing.

3) Although fluvial and tidal discharge respectively shape the morphology of the upper and lower NC reaches in general condition, episodic extreme floods can alter NC through smoothing the entire channel, which therefore also play an important role in the centennial morphological evolution of the NC.

While previous investigations on morphodynamic evolution of the Changjiang Estuary are still under debate, this study puts forward firstly that the upper and lower reaches of the NC showed distinct bathymetric variations at centennial scale in response to different natural forcings and anthropologic disturbances. Such insights can greatly enrich the estuarine science research and are highly significant to sustainable estuary management. We argue that taking pertinence measures in different areas of the estuary is a necessity for both the Changjiang Estuary and other similar mega estuaries under changing dynamic conditions.

Supplementary data to this article can be found online at https://doi.org/10.1016/j.geomorph.2017.11.014.

Uncited reference

Van der Wal et al., 2002

Acknowledgements

References

Anthony E.J., Marriner N. and Morhange C., Human influence and the changing geomorphology of Mediterranean deltas and coasts over the last 6000 years: from progradation to destruction phase?, *Earth-Sci. Rev.* **139**, 2014, 336–361.

Anthony E.J., Brunier G., Besset M., Goichot M., Dussouillez P. and Nguyen V.L., Linking rapid erosion of the Mekong River delta to human activities, *Sci. Rep.* **5**, 2015, 14745.

Bergillos R.J., Rodríguez-Delgado C., Millares A., Ortega-Sanchez M. and Losada M.A., Impact of river regulation on a Mediterranean delta: Assessment of managed versus unmanaged scenarios, *Water Resour. Res.* **52** (7), 2016, 5132–5148.

Blott S.J., Pye K., van der Wal D. and Neal A., Long-term morphological change and its causes in the Mersey estuary, NW England, *Geomorphology* **81**, 2006, 185–206.

Blum M.D. and Roberts H.H., Drowning of the Mississippi Delta due to insufficient sediment supply and global sea-level rise, *Nat. Geosci.* **2**, 2009, 488–491.

Burrough P.A. and McDonnell R.A., Principles of Geographical Information Systems, 1998, Oxford University Press, Oxford.

Chen J.Y., Yun C.X., Xu H.G. and Dong Y.F., The developmental model of the Chang Jiang River estuary during last 2000 years, *Acta Oceanol. Sin.* **1**, 1979, 103–111, (in Chinese with English abstract).

Chen Z.Y., Wang Z.H., Finlayson B., Chen J. and Yin D.W., Implications of flow control by the Three Gorges Dam on sediment and channel dynamics of the middle Yangtze (Changjiang) River, China, *Geology* **38** (11), 2010, 1043–1046.

Chu A., Wang Z. and Vriend H.J.D., Analysis on residual coarse sediment transport in estuaries, *Estuar. Coast. Shelf S.* **163**, 2015, 194–205.

Coco G., Zhou Z., van Maanen B., Olabarrieta M., Tinoco R. and Townend I., Morphodynamics of tidal networks: advances and challenges, *Mar. Geol.* **346**, 2013, 1–16.

Dai Z.J., Liu J.T., Fu G. and Xie H.L., A thirteen-year record of bathymetric changes in the north passage, Changjiang (Yangtze) estuary, *Geomorphology* **187** (4), 2013, 101–107.

Dai Z.J., Liu J.T., Wei W. and Chen J.Y., Detection of the Three Gorges Dam influence on the Changjiang (Yangtze River) submerged delta, *Sci. Rep.* **4**, 2014, 6600.

Dai Z.J., Liu J.T. and Wei W., Morphological evolution of the south passage in the Changjiang (Yangtze River) estuary, *China. Quatern. Int.* **380-381**, 2015, 314–326.

Dai Z., Fagherazzi S., Mei X., Chen J. and Meng Y., Linking the infilling of the north branch in the Changjiang (Yangtze) estuary to anthropogenic activities from 1958 to 2013, *Mar. Geol.* **379**, 2016a, 1–12.

Dai Z.J., Fagherazzi S., Mei X. and Gao J.J., Decline in suspended sediment concentration delivered by the Changjiang (Yangtze) River into the East China Sea between 1956 and 2013, *Geomorphology* **268**, 2016b, 123–132.

Dronkers J., Tidal asymmetry and estuarine morphology, *Neth. J. Sea Res.* **20** (2), 1986, 117–131.

Fagherazzi S., Carniello L., D'Alpaos L. and Defina A., Critical bifurcation of shallow microtidal landforms in tidal flats and salt marshes, *P. Natl. Acad. Sci. USA.* **103** (22), 2006, 8337–8341.

Garel E., Sousa C., Ferreira Ó. and Morales J.A., Decadal morphological response of an ebb-tidal delta and down-drift beach to artificial breaching and inlet stabilization, *Geomorphology* **216**, 2014, 13–25.

Jiang C.J., Li J.F. and de Swart H.E., Effects of navigational works on morphological changes in the bar area of the Yangtze estuary, *Geomorphology* **139-140**, 2012, 205–219.

Jiménez M., Castanedo S., Medina R. and Camus P., A methodology for the classification of estuary restoration areas: a management tool. Ocean coast, *Manage* **69**, 2012, 231–242.

Kim T.I., Choi B.H. and Lee S.W., Hydrodynamics and sedimentation induced by large scale coastal developments in the Keum River estuary, *Korea. Estuar. Coast. Shelf S.* **68** (3–4), 2006, 515–528.

Lai X., Yin D., Finlayson B.L., Wei T., Li M., Yuan W., Yang S., Dai Z., Gao S. and Chen Z., Will river erosion below the Three Gorges Dam stop in the middle Yangtze?, *J. Hydrol.* **554**, 2017, 24–31.

Lane A., Bathymetric evolution of the Mersey estuary, UK, 1906–1997: causes and effects, *Estuar. Coast. Shelf S.* **59**, 2004, 249–263.

Liu J.P., Xu K.H., Li A.C., Milliman J.D., Velozzi D.M., Xiao S.B. and Yang Z.S., Flux and fate of Yangtze River sediment delivered to the East China Sea, *Geomorphology* **85** (3–4), 2007, 208–224.

Liu J.T., Hsu R.T., Hung J.J., et al., From the highest to the deepest: the Gaoping River-Gaoping submarine canyon dispersal system, *Earth-Sci. Rev.* **153**, 2016, 274–300.

Luan H.L., Ding P.X., Wang Z.B., Ge J.Z. and Yang S.L., Decadal morphological evolution of the Yangtze estuary in response to river input changes and estuarine engineering projects, *Geomorphology* **265**, 2016, 12–23.

Luan H.L., Ding P.X., Wang Z.B. and Ge J.Z., Process-based morphodynamic modeling of the Yangtze estuary at a decadal timescale: controls on estuarine evolution and future trends, *Geomorphology* **290**, 2017, 347–364.

Mei X.F., Dai Z.J., Wei W. and Gao J.J., Dams induced stage–discharge relationship variations in the upper Yangtze River basin, *Hydrol. Res.* **47** (1), 2016, 157–170.

Miller J.K. and Dean R.G., Shoreline variability via empirical orthogonal function analysis: part I temporal and spatial characteristics, *Coast. Eng.* **54** (2), 2007, 111–131.

Mitchell S.B., Lawler D.M., West J.R. and Couperthwaite J.S., Use of continuous turbidity sensor in the prediction of fine sediment transport in the turbidity maximum of the Trent estuary, *UK. Estuar. Coast. Shelf Sci.* **58**, 2003, 645–652.

Nanson G.C. and Erskine W.D., Episodic changes of channels and floodplains on coastal rivers in New South Wales, In: Warner R.F., (Ed), *Fluvial Geomorphology of Australia*, 1988, Academic Press, Sydney, Australia.

Pye K. and Blott S.J., The geomorphology of UK estuaries: the role of geological controls, antecedent conditions and human activities, *Estuar. Coast. Shelf S.* **150**, 2014, 196–214.

Robins P.E., Skov M.W., Lewis M.J., et al., Impact of climate change on UK estuaries: a review of past trends and potential projections, *Estuar. Coast. Shelf S.* **169**, 2016, 119–135.

Sheng H., Dai Z.J., Mei X.F., Ge Z.P., Li S.S. and Gao J.J., Research on evolution and instability risk of the frontal river bed along the Qingcaosha reservoir, Changjiang estuary, *The Ocean Engineering* **35** (2), 2017, 105–114, (in Chinese with English abstract).

Simmons H.B., Some effects of upland discharge on estuarine hydraulics, *Proc. Amer. Soc. Civ. Eng.* **81** (792), 1955, 1–20.

Swenson J.B., Paola C., Pratson L. and Voller V.R., Fluvial and marine controls on combined subaerial and subaqueous delta progradation: morphodynamic modeling of compound clinoform development, *J. Geophys. Res.* **110**, 2005, F02013.

Syvitski J.P.M. and Saito Y., Morphodynamics of deltas under the influence of humans, *Global Planet. Chang.* **57**, 2007, 261–282.

Thomas C.G., Spearman J.R. and Turnbull M.J., Historical morphological change in the Mersey estuary, *Cont. Shelf Res.* **22**, 2002, 1775–1794.

Törnqvist T.E., Bick S.J., Klaas V.D.B. and De Jong A.F.M., How stable is the Mississippi Delta?, *Geology* **34** (8), 2006, 697–700.

Uncles R.J. and Stephens J.A., Dynamics of turbidity in the tweed estuary, *Estuar. Coast. Shelf Sci.* **45**, 1997, 745–758.

Van der Wal D., Pye K. and Neal A., Long-term morphological change in the Ribble estuary, northwest England, *Mar. Geol.* **189**, 2002, 249–266.

Wang Y., Ridd P.V., Wu H., Wu J. and Shen H., Long-term morphodynamic evolution and the equilibrium mechanism of a flood channel in the Yangtze estuary (China), *Geomorphology* **99**, 2008a, 130–138.

Wang H.J., Yang Z.S., Wang Y., Saito Y. and Liu J.P., Reconstruction of sediment flux from the Changjiang (Yangtze River) to the sea since the 1860s, *J. Hydrol.* **349** (3–4), 2008b, 318–332.

Wolanski E., Moore K., Spagnol S., D'Adamo N. and Pattiaratchi C., Rapid, human-induced siltation of the macro-tidal Ord River estuary, Western Australia, *Estuar. Coast. Shelf S.* **53**, 2001, 717–732.

Wright L.D. and Coleman J.M., Variations in morphology of major river deltas as a function of ocean waves and river discharge regimes, *Am. Assoc. Pet. Geol. Bull.* **57**, 1973, 177–205.

Wright L.D. and Coleman J.M., Mississippi River mouth processes: effluent dynamics and morphologic development, *J. Geol.* **82** (6), 1974, 751–778.

Yang S.L., Liu Z., Dai S.B., et al., Temporal variations in water resources in the Yangtze River (Changjiang) over the industrial period based on reconstruction of missing monthly discharges, *Water Resour. Res.* **46**, 2010, W10516.
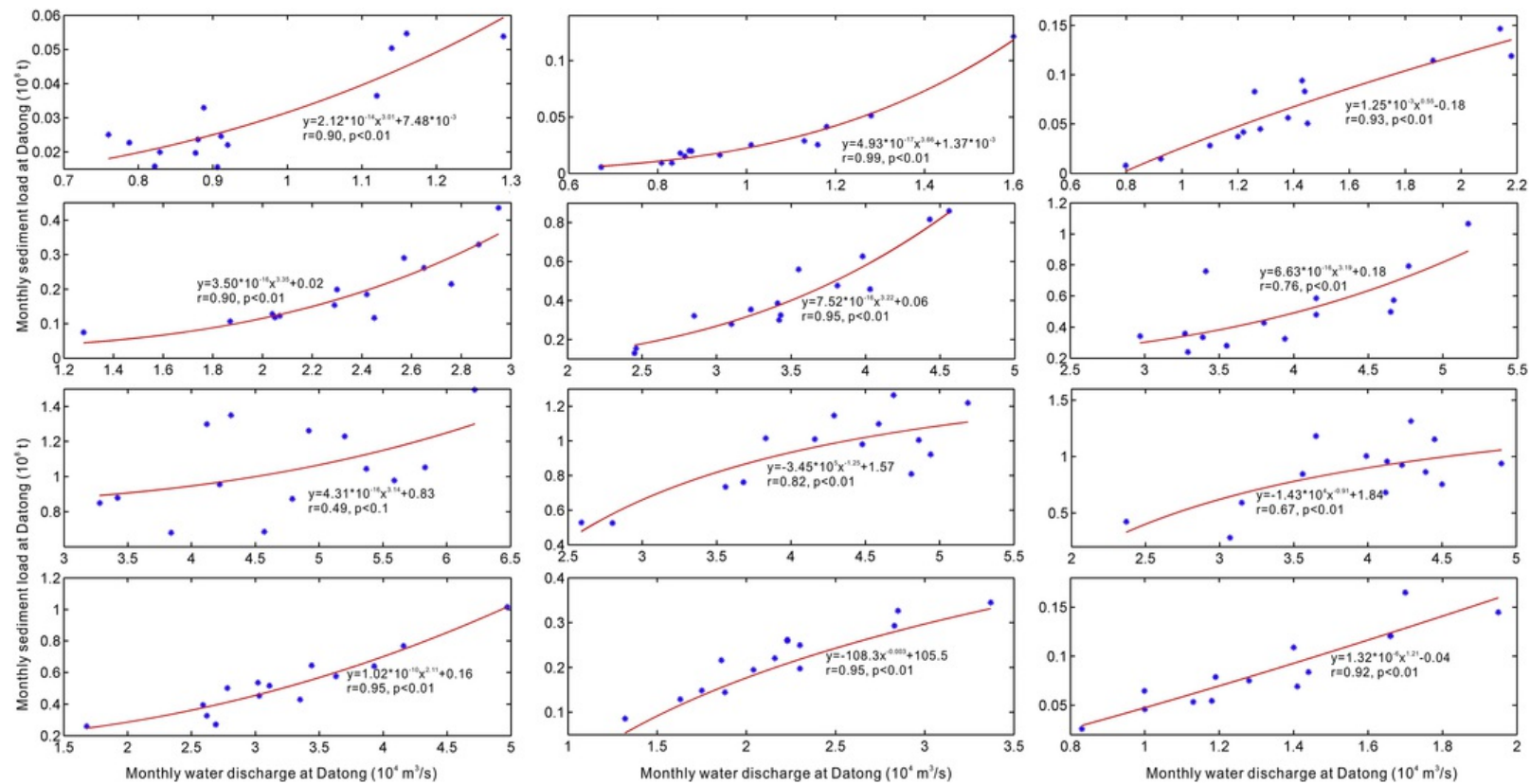
Yang S.L., Xu K.H., Milliman J.D., Yang H.F. and Wu C.S., Decline of Yangtze River water and sediment discharge: impact from natural and anthropogenic changes, *Sci. Rep.* **5**, 2015, 12581.

Monthly water discharge at Datong from 1865 to 1949 were reconstructed through a regression method (Yang et al., 2010). Specifically, for each month of the year, linear equations between the discharge at Hankou and Datong are established based on observations during the period 1950–2002 (Supplementary Fig. S1), excluding the effects of the TGD. Then the monthly discharge at Datong for the missing months (1865–1949) can be calculated using the regression equation with the corresponding observed discharge at Hankou. Monthly sediment discharge at Datong from 1865 to 1953 were reconstructed using a similar approach. Firstly, for each month of the year, power-law relationships to relate water sediment to water discharge were established for Datong station based on observations made during 1955–1968 (Supplementary Fig. S2), when the effects of human disturbance were nearly negligible (Wang et al., 2008b). The unknown monthly sediment loads from 1865 to 1953 were thereafter estimated through the rating curves and the corresponding monthly discharge. Thus the yearly water and sediment discharge can be extended to 1865–2013 by summing the monthly value.

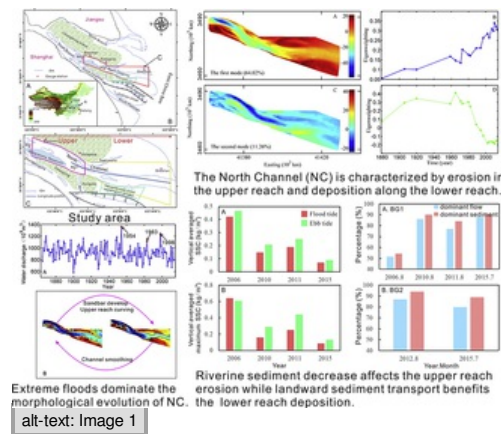The following are the supplementary data related to this article.

elsevier_GEOMOR_6229

Supplementary Fig. S1

elsevier_GEOMOR_6229
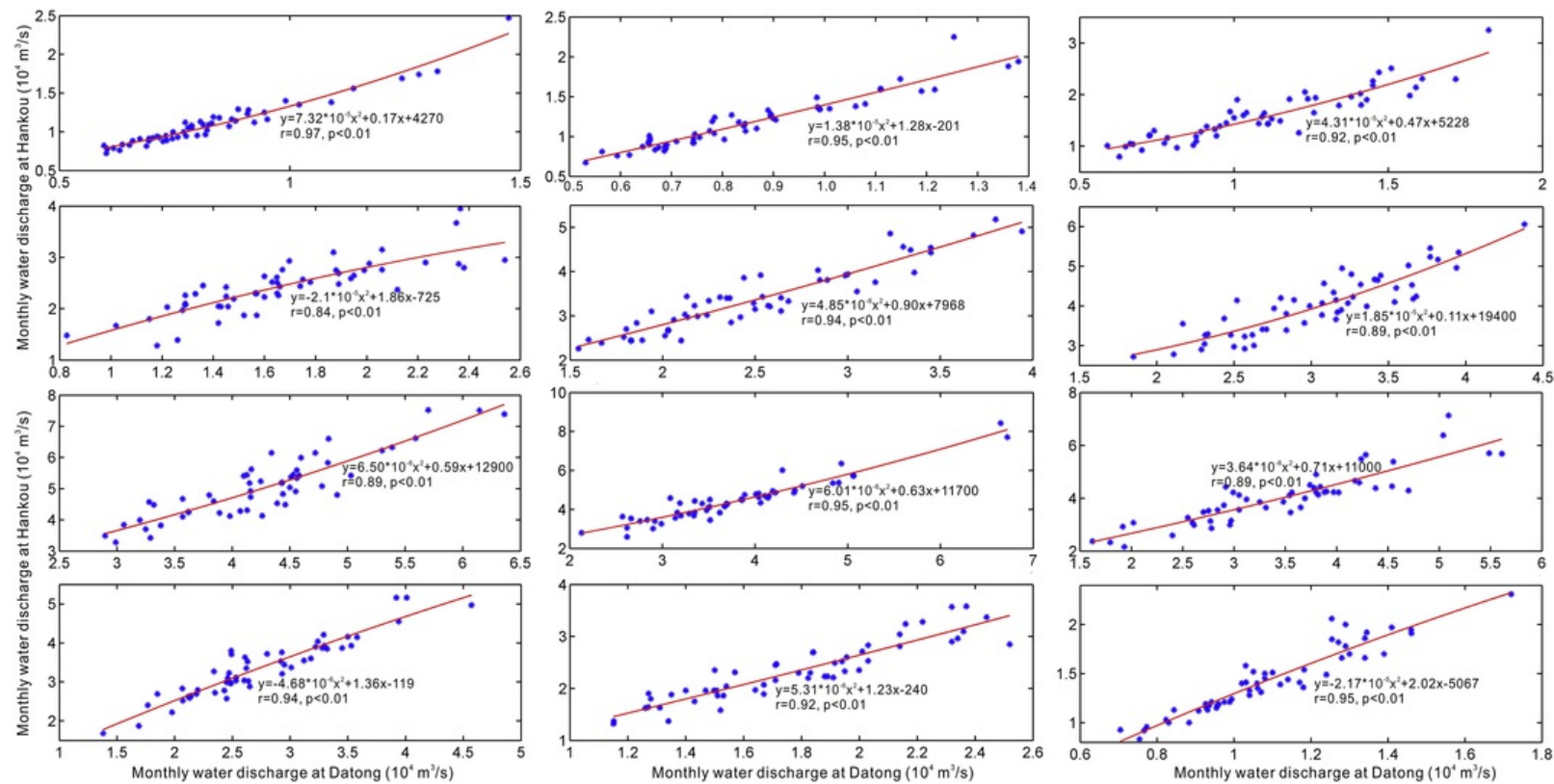
Supplementary Fig. S2

alt-text: Supplementary Fig. S2

Graphical abstract

alt-text: Image 1

Highlights

- NC is characterized by erosion in upper reach and deposition along the lower reach.
- Extreme floods dominate the episodic disequilibrium of NC evolution.
- Riverine and landward sediment availability control the NC morphology.
- Sediment trapping and water storage of TGD trigger the recent NC volume variation.

Queries and Answers

Query:

Your article is registered as a regular item and is being processed for inclusion in a regular issue of the journal. If this is NOT correct and your article belongs to a Special Issue/Collection please contact jaya.bhaskaran@elsevier.com immediately prior to returning your corrections.

Answer: Yes

Query:

Please confirm that given names and surnames have been identified correctly and are presented in the desired order, and please carefully verify the spelling of all authors' names.

Answer: Yes

Query:

The author names have been tagged as given names and surnames (surnames are highlighted in teal color). Please confirm if they have been identified correctly.

Answer: Yes

Query:

The citation "Dai et al., 2016" has been changed to "Dai et al., 2016a,b". Please check if appropriate and amend as necessary.

Answer: Thank you very much, the modification is correct. It should be "Dai et al., 2016a, b".

Query:

Citation "Chen et al., 2007" has not been found in the reference list. Please supply full details for this reference.

Answer: Sorry for our careless. The citation should be corrected to "Chen, 2007". The full details for this reference is: Chen J.Y., Research and practice of estuary and coast in China, 2007, Higher Education Press, Beijing, China.

Query:

The citation "Dai et al., 2016" has been changed to "Dai et al., 2016a, b" to match the author name/date in the reference list. Please check if the change is fine in this occurrence and modify the subsequent occurrences, if necessary.

Answer: Thank you very much. The change is fine.

Query:

The citation "Swenson, 2005" has been changed to "Swenson et al., 2005" to match the author name/date in the reference list. Please check if the change is fine in this occurrence and modify the subsequent occurrences, if necessary.

Answer: Highly appreciated. The change is fine.

Query:

Please provide caption for Supplementary Fig. S1.

Answer: The caption for Supplementary Fig. S1 is : The relationship between monthly water discharges at Datong and Hankou

Query:

Please provide caption for Supplementary Fig. S2.

Answer: The caption for Supplementary Fig. S2 is: The relationship between monthly water discharge and monthly sediment load at Datong

elsevier_GEOMOR_6229

Query:

Uncited reference: This section comprises references that occur in the reference list but not in the body of the text. Please position each reference in the text or, alternatively, delete it. Thank you.

Answer: Sorry for our careless. Please delete the uncited reference "Van der Wal et al., 2002" from the reference list. Thank you.